Simultaneous and Non-Simultaneous Drop Impact onto a Wall

Henrik Sontheimer[1], Leon Elsäßer[1], Peter Stephan[1], Tatiana Gambaryan-Roisman[1]
[1]Institute for Technical Thermodynamics, Technical University of Darmstadt
Peter-Grünberg-Straße 10, 64287 Darmstadt, Germany

ABSTRACT

In this work, we numerically investigate fluid dynamics during simultaneous and non-simultaneous impact of drops on a wall. Our goal is to improve the basic understanding of spray cooling, which is a promising method for cooling electronic components that dissipate heat with high heat flux. We vary the horizontal spacing and time interval between each drop to investigate their influences on the evolution of the wetted area, contact line length and liquid layer. Our study provides valuable insights into the complex fluid dynamics.

1. Introduction

Spray cooling is a promising method for managing high heat flux levels for electronic devices [1], but the understanding of the associated fluid dynamics and heat transport mechanisms is still incomplete [2].

In order to understand the fundamentals of spray cooling, previous studies have focused on a single drop impacting onto a wall [3]. However, studies devoted to interaction between two or several drops are rare [4].

In this work, we consider the impact in the parameter range, for which a single drop impact takes place in the drop deposition regime [3]. After impinging a substrate, the drop first undergoes a spreading phase, then a receding phase, and after several oscillations reaches a steady sessile drop phase. In this regime, experimental and numerical studies of heat transfer during a single drop impact have been performed, where, additionally, the temperature of the wall was set above the saturation temperature but below the onset of nucleate boiling [5, 6]. It has been shown that the maximal heat flow is reached during the spreading phase, in which the main mechanism of heat transport from the substrate to the fluid is heat convection. The role of evaporation increases during the spreading phase and becomes the main heat transport mechanism during the sessile phase. The heat flow increases and the wetted area decreases with increasing of wall superheat $\Delta T_\mathrm{w} = T_\mathrm{w} - T_\mathrm{sat}$, where T_w and T_sat describe wall and saturation temperature, respectively. These trends have also been observed experimentally by simultaneous or nearly-simultaneous impact of two drops onto close locations of a superheated wall [4, 7, 8].

The simultaneous and non-simultaneous impact of two drops onto two close locations may lead to coalescence of the drops and to formation of an uprising liquid sheet along the intersection line of the drops. This sheet is inclined towards the earlier impinged drop for non-simultaneous drop impact. The height of the liquid sheet is maximal at its center [9, 10]. The horizontal coalescence leads to decrease of the wetted area and to decrease of the heat flow compared to two non-interacting drops, and thus to reduced cooling efficiency [4, 7, 11]. The heat transfer decreases with decreasing of spacing parameter $e = d/D_0$, where d and D_0 describe horizontal distance of the drop centers and initial drop diameter, respectively [7, 8, 9, 11].

Gholijani et al. [7] have shown that increasing the time interval at which two drops impact with identical impact velocity one after the other, leads to a decrease in the maximum heat flux transferred. However, the total accumulated heat removed from the substrate over the time interval is hardly affected. Benther et al. [4] observed reduced cooling performance in the case of non-simultaneous drop impact ($\delta t > 0$) compared to simultaneous drop impact ($\delta t = 0$).

In their numerical study, Ashoke Raman et al. [12] varied the impact velocity of one of the two drops to describe a non-simultaneous impact with a time interval δt between the two drops. They identified out-of-phase (small time interval) and in-phase (large time interval) coalescence modes. Thereby, the interacting liquid rims move in the same or opposite direction, respectively. However, the results reported in [12] do not allow to separate the effects of the difference in impact velocities and of the time interval δt on flow dynamics.

The heat transfer rate during impact of one or more drops depends not only on the wetted area, but also on the length of the three-phase contact line, where solid, liquid, and vapor meet [5, 6]. It has been observed that the heat flow significantly increases with the length of the contact line [7, 11, 13].

From the literature review it can be concluded that there is no numerical study on the influence of the time interval, $\delta t > 0$, on flow dynamics of two drops impinging a surface with an equal velocity. In the present work, the flow dynamics during horizontal coalescence of two drops impacting a substrate with an equal velocity in the drop deposition regime is studied numerically. Heat transfer is not taken into account at this stage. The influence of the spacing parameter and time interval on the evolution of wetted area and the contact line length is studied. These results provide a perspective on the heat transfer behavior.

2. Numerical Method

We use the incompressible `interFlow` solver from the TwoPhaseFlow library [14] within OpenFOAM based on the finite volume method. A detailed description of the numerical framework can be found in [14, 15].

The simulations are performed with a constant contact angle of 30°. This contact angle corresponds to the static contact angle at a wall superheat of $\Delta T_\mathrm{w} = 7.3\,\mathrm{K}$ determined by the micro region model [16] for refrigerant perfluorohexane (FC-72) and a calcium fluoride wall. This choice enables comparison with experiments [7].

Corresponding author: Henrik Sontheimer
E-mail address: sontheimer@ttd.tu-darmstadt.de

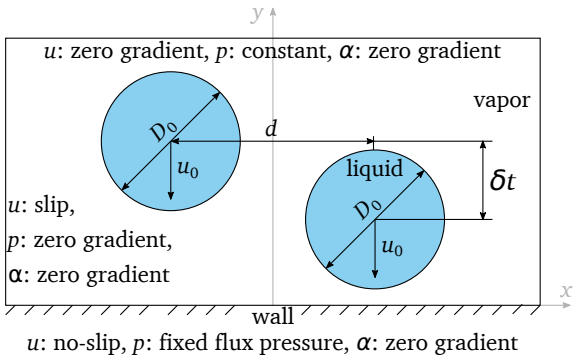

Fig. 1 Initial and boundary conditions for the case of non-simultaneous drop impact (not to scale). The axis z is normal to the plane of the picture. Boundary conditions at the right and back patch are set identical to the boundary condition at the left patch. Front patch is set to symmetry.

2.1 Governing Equations

We use the Volume-of-Fluid method to track the liquid-vapor interface. Thus, the conservation equation for the volume fraction,

$$\frac{\partial \alpha}{\partial t} + \nabla \cdot (u\alpha) = 0, \tag{1}$$

is solved, where u describes the velocity. The volume fraction α describes the ratio of liquid volume within a cell to the cell volume [14].

Additionally, the conservation equations for mass and momentum are solved,

$$\nabla \cdot u = 0, \tag{2}$$

$$\rho \left(\frac{\partial u}{\partial t} + (u \cdot \nabla) u \right) = -\nabla p_{\mathrm{rgh}} + \mu \nabla^2 u + f_g + f_\sigma, \tag{3}$$

where μ and p_{rgh} describe dynamic viscosity and pressure, respectively. All fluid properties are averaged using the volume fraction. The source terms f_g and f_σ account for gravity and surface tension [14].

2.2 Numerical Setup

Figure 1 shows the computational domain as well as the initial and boundary conditions. In the case of simultaneous drop impact, only half of the domain is used due to additional symmetry plane. The second drop is initialized by overwriting the volume fraction and velocity fields within the second drop after the time interval δt has passed.

Similar to experiments [7], the drop is initialized with an initial drop diameter of $D_0 = 0.93\,\mathrm{mm}$ and an impact velocity of $u_0 = 0.5\,\mathrm{m\,s^{-1}}$. Fluid properties are defined for refrigerant perfluorohexane (FC-72) at saturation conditions ($p_{\mathrm{sat}} = 0.94\,\mathrm{bar}$). The corresponding Reynolds ($Re = \rho_{\mathrm{l}} D_0 u_0 \mu_{\mathrm{l}}^{-1}$), Weber ($We = \rho_{\mathrm{l}} D_0 u_0^2 \sigma^{-1}$) and Bond ($Bo = 0.25 \rho_{\mathrm{l}} g D_0^2 \sigma^{-1}$) numbers are $Re = 1700$, $We = 49$ and $Bo = 0.4$, respectively.

We use a static, hexahedral mesh with a mesh refinement from $\Delta x_{\mathrm{max}} = 80\,\mu\mathrm{m}$ to $\Delta x_{\mathrm{min}} = 5\,\mu\mathrm{m}$. The time step is adjusted similar to [16] using the Courant number and the criterion from Brackbill et al. [17].

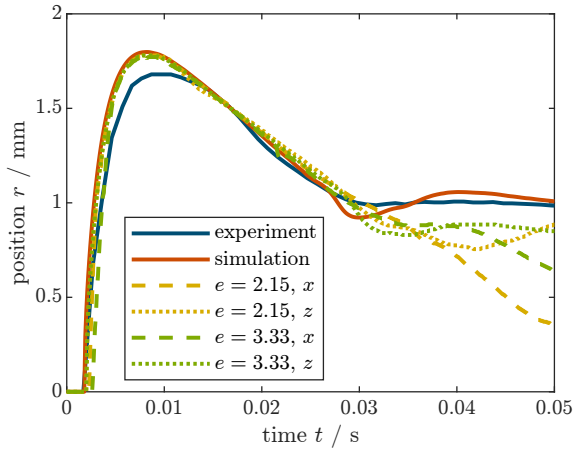

Fig. 2 Temporal evolution of the contact line radius. Impact parameters for simulation of the single drop impact according to Sec. 2.2, experiments with similar impact parameters from [6] ($u_0 = 0.44\,\mathrm{m\,s^{-1}}$, $\Delta T_{\mathrm{w}} = 6.9\,\mathrm{K}$). Dashed and dotted lines show the evolution of the contact line position in x- and z-direction for the case of simultaneous drop impact (see Fig. 3).

3. Results and Discussion

First, we validate our numerical model by comparing the numerical predictions for the case of the single drop impact to similar experiments from [6]. Figure 2 shows a good agreement between simulations and experiments for the temporal evolution of the contact line radius. This is despite the neglect of heat transfer and the use of a constant contact angle in our model.

Our numerical model slightly overpredicts the maximum contact line radius, and oscillations after the receding phase are slightly more pronounced compared to the experiment.

Next, we study the simultaneous drop impact for two different spacing parameters, $e = 2.15$ and $e = 3.33$. In Fig. 2 we analyze the temporal evolution of the contact line position in x- and z-direction. The non-interacting part of the liquid rim of the drop is only influenced by the coalescence after the receding phase of the single drop has ended. In the case of horizontal coalescence, the receding continues since the coalesced drops form a single sessile drop. The behavior of the non-interacting part of the rim was already observed in experiments [7] and simulations [11]. Note that in spray cooling applications all parts of the liquid rim are typically influenced by the interaction with neighboring drops.

For the case of $e = 2.15$, we consider four time intervals: $\delta t = 0$, 4, 15 and 30 ms, corresponding to simultaneous drop impact, out-of-phase coalescence, in-phase coalescence and impact during the sessile drop phase of the initial drop, respectively. Figure 3 illustrates the flow dynamics in these four cases. In the case of simultaneous drop impact ($\delta t = 0\,\mathrm{ms}$), a straight, wide liquid sheet forms between the two coalescing drops. The drop spreading and receding is symmetrical. In case of out-of-phase coalescence ($\delta t = 4\,\mathrm{ms}$), we observe a wide, semi-lunar shaped uprising liquid sheet. During the spreading of the second drop ($t_{\mathrm{ref}} = 3\,\mathrm{ms}$), capillary waves travel over the initial drop and a liquid tip forms at the sides of the uprising liquid sheet. Here, this tip is even more

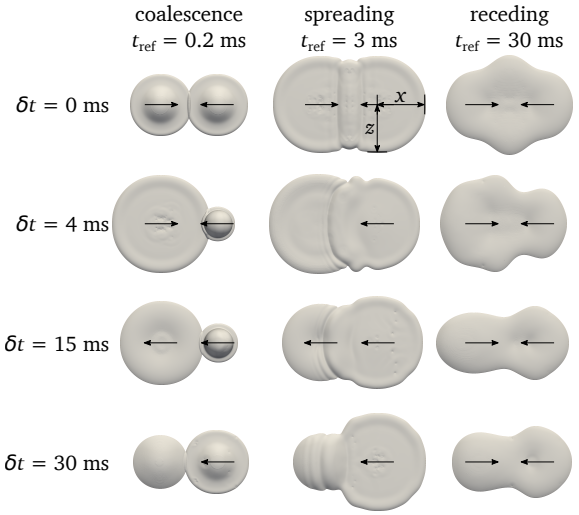

Fig. 3 Top view (x-z-plane) for $e = 2.15$ and various time intervals δt just after first drop interaction ($t_{ref} = 0.2$ ms), during spreading of the first drop ($t_{ref} = 3$ ms) and during receding of the coalesced drop ($t_{ref} = 30$ ms). The time of first drop interaction is set to $t_{ref} = 0$ ms.

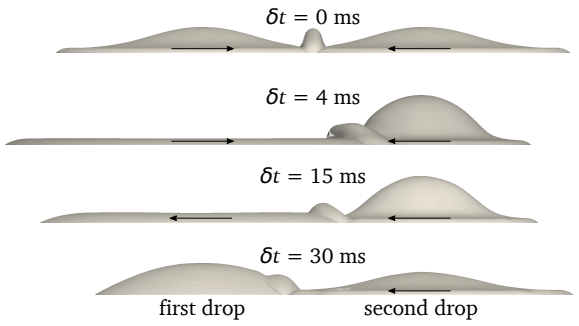

Fig. 4 Side view (x-y-plane) at 0.8 ms after the first drop interaction for $e = 2.15$ and various time intervals δt.

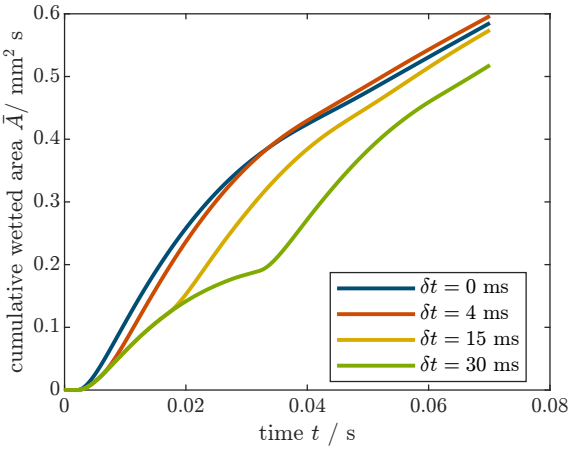

Fig. 5 Temporal evolution of the cumulative wetted area for the case of $e = 2.15$ and various time intervals δt.

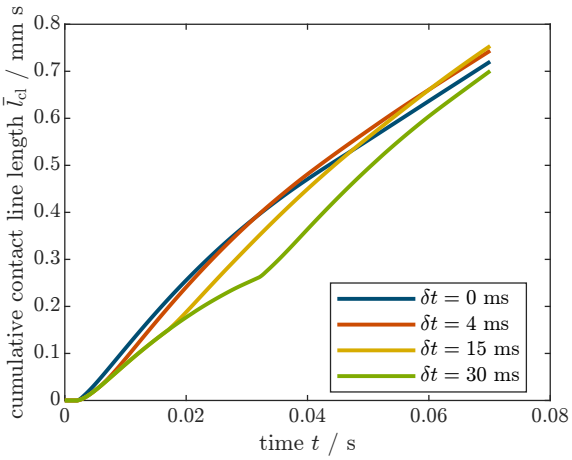

Fig. 6 Temporal evolution of the cumulative contact line length for the case of $e = 2.15$ and various time intervals δt.

pronounced compared to the case of simultaneous drop impact. The receding behavior ($t_{ref} = 30$ ms) is asymmetric. During both in-phase coalescence ($\delta t = 15$ ms) and impact during the sessile drop phase ($\delta t = 30$ ms), the second drop spreads over the first drop. Again, we observe a semi-lunar uprising liquid sheet and an asymmetric receding behavior. However, the liquid sheet is not as wide as in the case of out-of-phase coalescence and no liquid tips at the side are formed. In all cases, finally, one large, sessile single drop is formed.

Figure 4 shows the side view of the coalescence process. For simultaneous drop impact ($\delta t = 0$ ms), the uprising liquid sheet is straight. However, for non-simultaneous drop impact ($\delta t > 0$ ms), the liquid sheet is inclined towards the earlier impinged drop.

If the drops impinge a superheated wall at a temperature below the onset of nucleate boiling, the heat transport from the wall to the fluid is governed by the wetted area and the length of the contact line [5, 6]. Hence, we can give a perspective on the heat transfer by analyzing the temporal evolution of the cumulative wetted area and cumulative contact line length.

Figure 5 shows the cumulative wetted area over time. Despite very different spreading behavior and different maximum wetted area, the cumulative wetted area over time behaves almost identical for all cases in the long run. Only the case of drop impact during the sessile drop phase ($\delta t = 30$ ms) performs worse. This is because the second drop impinges at a later time instant resulting in less liquid volume wetting the wall at earlier time instants.

The cumulative contact line length behaves similarly to the cumulative wetted area, as it is shown in Fig. 6. Only in the case of in-phase coalescence ($\delta t = 15$ ms) the cumulative contact line performs slightly better than the wetted area.

As a result, we expect the overall transferred heat to be similar in all cases independent of the time interval. The trend in the cumulative wetted area agrees well with the heat transfer behavior from Gholijani et al. [7], who concluded that the overall transferred heat is almost independent of the time interval. Our predictions regarding cumulative wetted area also agrees with the findings from Benther et al. [4], since our trend shows a slight increase in wetted area with decreasing time interval for the case of non-simultaneous drop impact ($\delta t > 0$ ms).

4. Conclusions

In order to enhance the understanding of spray cooling we have conducted a numerical study on the simultaneous and non-simultaneous drop impact onto a wall. In a first step, we have neglected heat transport in our model. The main findings are:

- During horizontal coalescence, the non-interacting part of the rim behaves similarly to the single drop impact until the end of its receding phase.
- The uprising liquid sheet is straight in case of simultaneous drop impact and has a semi-lunar shape inclined towards the earlier impinged drop in case of non-simultaneous drop impact.
- Despite different maximum wetted area and asymmetric receding behavior, the cumulative wetted area as well as the cumulative contact line length are almost independent of the time interval between the drops.
- This trend gives a perspective on heat transfer and agrees well with findings from literature for horizontal coalescence on a superheated wall.

In upcoming studies, we will consider heat transport in our numerical model to study simultaneous and non-simultaneous drop impact onto a superheated wall.

Acknowledgments

We kindly acknowledge the financial support of the Deutsche Forschungsgemeinschaft (DFG, German Research Foundation) – Project SFB-TRR 75, Project number 84292822.

This article was written as part of the LoTuS project (funding code 03EN2026), which is funded by the Bundesministerium für Wirtschaft und Klimaschutz (BMWi, German Federal Ministry for Economic Affairs and Climate Protection) and supervised by the project executing organization Jülich.

Calculations for this research were conducted on the Lichtenberg high-performance computer at the Technical University of Darmstadt.

References

[1] J. Kim, *Int. J. Heat Fluid Flow*, 28, (2007), 753–767.

[2] J.D. Benther, J.D. Pelaez-Restrepo, C. Stanley, G. Rosengarten, *Int. J. Heat Mass Transf.*, 178, (2021), 121587.

[3] J. Breitenbach, I.V. Roisman, C. Tropea, *Exp. Fluids*, 59, (2018), 55.

[4] J.D. Benther, V. Bhatt, J.D.P Restrepo, C. Stanley, G. Rosengarten, *Int. J. Heat Mass Transf.*, 191, (2022), 122752.

[5] S. Herbert, S. Fischer, T. Gambaryan-Roisman, P. Stephan, *Int. J. Heat Mass Transf.*, 178, (2017), 605–614.

[6] A. Gholijani, C. Schlawitschek, T. Gambaryan-Roisman, P. Stephan, *Int. J. Heat Mass Transf.*, 153, (2020), 119661.

[7] A. Gholijani, T. Gambaryan-Roisman, P. Stephan, *Exp. Therm. Fluid Sci.*, 131, (2022), 110520.

[8] A. Gultekin, N. Erkan, E. Ozdemir, U. Colak, S. Suzuki, *Exp. Therm. Fluid Sci.*, 120, (2021), 110255.

[9] I.V. Roisman, B. Prunet-Foch, C. Tropea, M. Vignes-Adler, *J. Colloid Interface Sci.*, 256, (2002), 396–410.

[10] N.E. Ersoy, E. Morteza, *Phys. Fluids*, 32, (2020), 012108.

[11] S. Batzdorf, J. Breitenbach, C. Schlawitschek, I.V. Roisman, C. Tropea, P. Stephan, T. Gambaryan-Roisman, *Int. J. Heat Mass Transf.*, 113, (2017), 898–907.

[12] K. Ashoke Raman, R.K. Jaiman, T. Lee, H. Low, *J. Colloid Interface Sci.*, 486, (2017), 265–276.

[13] M. Winter, *Dissertation*, TU Darmstadt, (2015), `http://tuprints.ulb.tu-darmstadt.de/4041/`.

[14] H. Scheufler, J. Roenby, *arXiv*, (2021), `https://arxiv.org/abs/2103.00870`.

[15] H. Scheufler, J. Roenby, *J. of Comp. Phys.*, 383, (2019), 1–23.

[16] S. Batzdorf, *Dissertation*, TU Darmstadt, (2015), `http://tubiblio.ulb.tu-darmstadt.de/73268/`.

[17] J.U. Brackbill, D.B. Kothe, C. Zemach, *J. Comput. Phys.*, 100, (1992), 335–354.